Cell Reports
Article

Plac8 Links Oncogenic Mutations to Regulation of Autophagy and Is Critical to Pancreatic Cancer Progression

Conan Kinsey,[1,5] Vijaya Balakrishnan,[1,5] Michael R. O'Dell,[2] Jing Li Huang,[2] Laurel Newman,[1] Christa L. Whitney-Miller,[3] Aram F. Hezel,[2,4,*] and Hartmut Land[1,4,*]
[1]Department of Biomedical Genetics
[2]Department of Medicine
[3]Department of Pathology and Laboratory Medicine
[4]James P. Wilmot Cancer Center
University of Rochester Medical Center, 601 Elmwood Avenue, Rochester, NY 14642, USA
[5]Co-first author
*Correspondence: aram_hezel@urmc.rochester.edu (A.F.H.), land@urmc.rochester.edu (H.L.)
http://dx.doi.org/10.1016/j.celrep.2014.03.061

SUMMARY

Mutations in *p53* and *RAS* potently cooperate in oncogenic transformation, and correspondingly, these genetic alterations frequently coexist in pancreatic ductal adenocarcinoma (PDA) and other human cancers. Previously, we identified a set of genes synergistically activated by combined *RAS* and *p53* mutations as frequent downstream mediators of tumorigenesis. Here, we show that the synergistically activated gene *Plac8* is critical for pancreatic cancer growth. Silencing of *Plac8* in cell lines suppresses tumor formation by blocking autophagy, a process essential for maintaining metabolic homeostasis in PDA, and genetic inactivation in an engineered mouse model inhibits PDA progression. We show that Plac8 is a critical regulator of the autophagic machinery, localizing to the lysosomal compartment and facilitating lysosome-autophagosome fusion. *Plac8* thus provides a mechanistic link between primary oncogenic mutations and the induction of autophagy, a central mechanism of metabolic reprogramming, during PDA progression.

INTRODUCTION

Pancreatic ductal adenocarcinoma (PDA) depends on a marked reprogramming of metabolic pathways, including the acquisition of autophagy dependence, for tumor cell survival and growth (Guo et al., 2011; Lock et al., 2011; Yang et al., 2011; Ying et al., 2012). Autophagy (or macroautophagy) is the process of autodigestion that recycles damaged organelles and enables cells to combat oxidative and nutrient stress and appears to have a context-dependent role in cancer. A present model suggests that autophagy has a dual role in cancer; suppressing cancer progression at its earliest stages, while allowing advanced cancers to meet metabolic demands (Kimmelman, 2011; White, 2012). Consistent with this, PDA and other tumor cell lines show constitutive basal autophagy in normal growth media, and pharmacologic or genetic blockade of autophagy strongly impairs tumor growth of xenograft models (Guo et al., 2011; Lock et al., 2011; O'Dell et al., 2012; Yang et al., 2011).

The spectrum of mutational events in PDA is well defined with activating RAS mutations present in most tumors (93%) and common inactivating mutational events in *TP53*, *CDKN2A*, and *SMAD4* tumor suppressors and associated pathway components (Biankin et al., 2012). Analysis of human PDA pathological precursors, together with studies in genetically engineered mice, have established activating *RAS* mutations as a critical early events in PDA pathogenesis with cooperating loss of tumor suppressors genes occurring later (Aguirre et al., 2003; Bardeesy et al., 2006a; Hingorani et al., 2003; Hruban et al., 2001). How these mutational events in PDA cause autophagy dependence and the timing of autophagy activation in the course of cancer progression have not been established. Among the commonly mutated genes in PDA, *RAS* has been associated with autophagy activation, though not all *RAS* mutant tumor demonstrate autophagy dependence (Guo et al., 2011; Yang et al., 2011). Inactivation of the *p53-p19Arf* tumor suppressor axis has also been implicated in autophagy control with differing effects depending on the experimental context (Balaburski et al., 2010; Feng et al., 2005; Pimkina and Murphy, 2009; Tasdemir et al., 2008). The roles of these primary oncogenic mutations in causing autophagy activation in PDA, and a molecular basis for this phenomenon, thus remain unclear.

Previously, we have shown that genes regulated synergistically in response to common cooperating oncogenic mutations found in PDA (*RAS* activation and functional loss of *p53*) are causally linked to the cancer phenotype. These genes, termed "cooperation response genes" (CRGs), encompass a spectrum of cellular processes down-stream of oncogenic mutations that are required for RAS/p53-mediated tumorigenesis (McMurray et al., 2008; Smith and Land, 2012). Here, we show that one such CRG, Plac8 is upregulated by cooperating RAS and p53

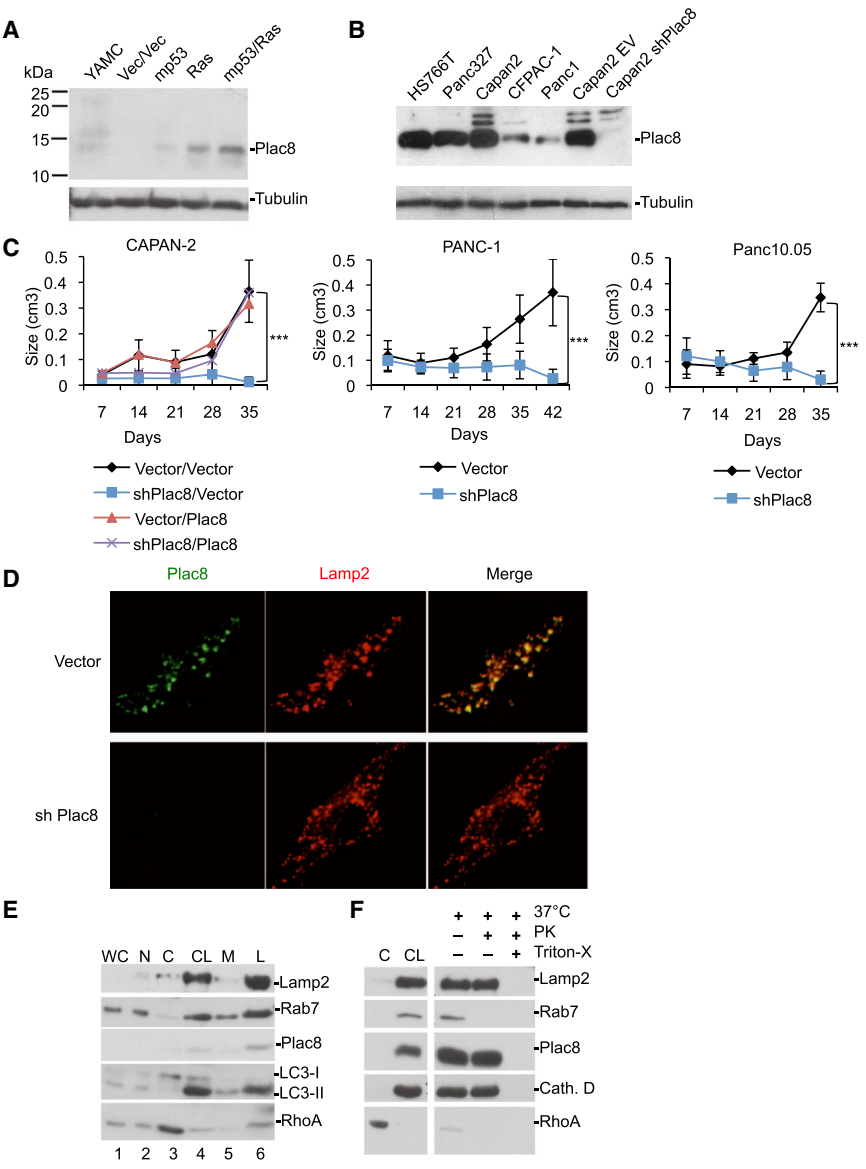

Figure 1. Plac8 Expression Induced by Oncogenic Mutations Is Critical for Growth of Human Xenograft PDA Cell Lines and Is Localized to the Lysosome Compartment

(A) Immunoblotting of murine YAMC, vector, mp53, Ras, and mp53/Ras transformed cells with anti-Plac8 antibody.

(B) Immunoblotting of human PDA cell lines including CAPAN-2 cells stably infected with *Plac8* shRNA expressing vector or control with anti-Plac8 antibody and β-tubulin (loading control).

(C) Vector control and *Plac8* KD CAPAN-2 cells were injected into CD-1 nude mice, and vector control and *Plac8* KD PANC-1 and Panc10.05 cell lines were injected into NOD/SCID mice. Data are presented as means ± SD (significance by Student's t test, ***$p < 0.001$).

(D) mp53/Ras murine cells were fixed and stained using anti-Plac8 and anti-Lamp2 antibodies and imaged by confocal microscopy.

(E) Subcellular fractionation and immunoblotting of mp53/Ras transformed murine cells for Plac8, lysosomal proteins Rab7 and Lamp2, autophagosomal protein LC3, and a cytosolic control RhoA. Lanes are as follows: WC (1): whole-cell lysate, N(2): nuclear fraction, C(3): cytosolic fraction, CL(4): crude lysosomal fraction, M(5): microsomal fraction, L(6): lysosomal fraction.

(F) Cytosolic fractions (C) and crude lysosomal fractions (CL) were isolated from mp53/Ras murine cells and the crude lysosomal fraction subjected to a Proteinase K protection assay. Lysosomes were treated with Proteinase or treated with Proteinase K and Triton X-100 to dissolve the lysosomal membrane and immunoblotted for the external lysosomal protein Rab7, internal lysosomal proteins Lamp2 and Cathepsin D, and Plac8. RhoA served as a cytosolic fraction control.

mutations in PDA and critical to the growth of RAS/p53 mutant tumors by sustaining autophagy, via enabling autophagosome-lysosome fusion. Thus Plac8 provides a mechanistic link between the cooperation of two common pancreatic cancer causing gene mutations, *KRAS* and *p53*, and the elevated rates of autophagy critical to tumor growth.

RESULTS

Plac8 Expression Is Induced in Response to *Ras* and *p53* Mutations and Is Critical for Pancreatic Tumor Growth

We have previously identified Plac8, a 112-amino-acid cysteine-rich protein that is upregulated at the RNA level in PDA (Buchholz et al., 2005; Lowe et al., 2007), as critical to malignant cell transformation mediated by activated *RAS* (RasV12) and mutant *p53* (mp53) (McMurray et al., 2008). The biochemical function of Plac8 is unknown, but the gene has been linked to efficient killing of phagocytosed bacteria by neutrophils, where it is enriched in a modified form of lysosomes, known as the granular fraction, critical for intracellular antimicrobial action (Ledford et al., 2007). We confirmed that Plac8 protein levels are induced synergistically in response to combined expression of *mp53* and *RasV12* in young adult mouse colon (YAMC) cells (Figure 1A) and can be detected in human pancreatic cancer cell lines (Figure 1B). Notably, we found that small hairpin RNA (shRNA)-mediated knockdown of Plac8 virtually abolished tumorigenicity of the CAPAN-2, Panc-1, and Panc10.05 human PDA cell lines implanted into immunocompromised mice (Figures 1C and S1). Thus, Plac8 is cooperatively induced in response to mutations in *RAS* and *p53* and is essential for the cancer phenotype of human PDA cell lines.

Plac8 Is Predominantly Located to the Lysosome

The subcellular location of Plac8 in epithelial cells was established by immunostaining of mp53/Ras cells with Plac8-specific antibodies, which showed predominantly punctate perinuclear

staining sensitive to Plac8 knockdown and partial colocalization with staining for the lysosomal protein Lamp2 (Figure 1D). Correspondingly, subcellular fractionation experiments indicated enrichment of Plac8 protein together with lysosomal proteins Lamp2 and Rab7 (Figure 1E) (Eskelinen et al., 2002; Gutierrez et al., 2004; Huynh et al., 2007; Jäger et al., 2004). As observed for the intralysosomal proteins Lamp2 and Cathepsin D, Plac8 is resistant to proteinase K digestion, whereas the external lysosomal protein Rab7 is degraded (Figure 1F). Thus, in epithelial cells, Plac8 appears to be a predominantly intravesicular protein, with significant localization to the lysosomal compartment.

Plac8 Facilitates Autophagosome-Lysosome Fusion

Autophagy is induced upon nutrient stress in normal cells, whereas in PDA cells autophagy is constitutively activated in the presence of nutrients (Yang et al., 2011). The mediators of this activation are unknown. As key late steps of autophagy involve autophagosome maturation and lysosomal fusion leading to autolysosome formation, we hypothesized that the localization of Plac8 to lysosomes may relate to a role in autophagy. In particular, we wished to address whether Plac8 regulates lysosomal function and/or fusion with degradative endosomes, such as phagosomes (as is the case for Plac8 function in neutrophils) or autophagosomes. To test the impact of Plac8 on AL fusion, we compared colocalization of the GFP-labeled microtubule associated protein 1 light chain 3 (LC3), a marker of autophagy that associates with the autophagosome membrane after processing (Klionsky et al., 2008), and the lysosomal marker Lamp2 in control and Plac8 knockdown (KD) cells by confocal analysis (Morselli et al., 2010). Plac8 KD resulted in an ~80% reduction in GFP-LC3/Lamp2 colocalization in murine mp53/Ras cells and CAPAN-2 PDA cells indicating a reduction in AL fusion (Figures 2A and 2B). This effect was specific to the reduction in Plac8 levels, because fusion was rescued by the expression of an shRNA-resistant Plac8 in either cell type (Figures 2A and 2B). Moreover, consistent with our interpretation that Plac8 facilitates AL fusion Plac8 KD resulted in accumulation of autophagy markers p62 and LC3 both in normal growth medium and in nutrient-depleted HBSS (Figures 2C and 2D), with p62 and LC3 reverting to control levels in presence of a shRNA-resistant Plac8 protein (Figures 2E and 2F).

Diminished AL fusion following Plac8 KD should lead to a reduction in autophagic flux as indicated by accumulation of autophagosomes. This was confirmed using the mCherry-EGFP-LC3 reporter as a probe to estimate the relative numbers of autophagosomes and autolysosomes, as indicated by yellow (green+red) and red fluorescence, respectively (Kimura et al., 2007) in both normal growth medium and in nutrient-depleted conditions (Figure 2G). In addition, transmission electron microscopy revealed induction of vesicular structures enveloped by multiple membranes harboring cytosolic content consistent with accumulated autophagosomes in Plac8 knockdown (KD) cells that were only rarely found in vector control cells (Figure S2).

Further evidence indicating a role of Plac8 in facilitating autophagic flux comes from experiments in which we introduced exogenous Plac8 into YAMC cells expressing activated *Ras*. Exogenous Plac8 diminished the abundance of autolysosomes, as indicated by decreased red fluorescence of the mCherry-EGFP-LC3 reporter (Figure S3A). In addition, levels of endogenous p62 and LC3II proteins were diminished in reporter-free cells (Figure S3B). In contrast, all these indicators accumulated to levels above controls in presence of chloroquine (CQ), an inhibitor of lysosomal function acting via alkalinization of lysosomal pH (Klionsky et al., 2012) (Figures S3A and S3B). Similarly, both the numbers of endogenous LC3 puncta and their colocalization with Lamp2 increased significantly in presence of CQ and exogenous Plac8 (Figure S3C). Together, this suggests a scenario in which Plac8 facilitates autophagic flux. Plac8 expression has minimal impact on p62 and LC3II protein levels in parental YAMC cells and in mp53 cells, i.e., YAMC cells expressing mutant p53 in absence of activated Ras (Figures S3D and S3E). Plac8 thus collaborates with activated Ras to elevate autophagic flux, though this is not sufficient to cause tumor growth in mice (Figure S3F).

AL fusion requires the Ras-like GTPase Rab7 and is blocked by Rab7-T22N, a dominant-negative mutant (Rab7DN), thus leading to autophagosome accumulation (Ganley et al., 2011; Gutierrez et al., 2004; Jäger et al., 2004). Similarly, we found that expression of Rab7DN prevented tumor growth in murine and human tumor cells, while inducing both accumulation of p62 and LC3 and decreased colocalization of Lamp2 and GFP-LC3 (Figures 3A, 3B, and 4), consistent with a block in AL fusion. In contrast, expression of a dominant-negative mutant of Rab5a, a gene critical to early endocytosis/phagocytosis (Bucci et al., 1992; Chen and Wang, 2001; Dinneen and Ceresa, 2004), did not impact AL fusion, p62, or LC3 levels indicating that inhibition of Rab5a signaling, and early endocytosis did not effect autophagy (Figures 3C, 3D, 4A, and 4B). As expected, Rab5aDN inhibited endocytosis, as indicated by a decrease in uptake of fluorescently labeled dextran in the same cells, further suggesting that Rab5a-mediated endocytosis is nonessential for the tumor growth among these cells (Figure S4).

Given the phenotypic similarities in the effects of Plac8 and Rab7 on autophagy and in promoting AL fusion, we sought to determine if Rab7 activation could overcome the effects of Plac8 KD. Exogenous expression of dominant-active Rab7 Q67L (Rab7DA) in the presence of Plac8 KD reversed the tumor-inhibitory effect of Plac8 knockdown (Figures 3E and 3F), increased Lamp2 and GFP-LC3 colocalization (Figures 4A and 4B), and led to diminished levels of p62 and LC3 (Figures 3E and 3F), indicative of rescued AL fusion and autophagosomal processing. The ability of Rab7DA alone to inhibit tumor formation may thus be due to overactivation of autophagy, an effect compensated in the presence of Plac8 knockdown (Figures 3E and 3F).

In summary, our data indicate that knockdown of Plac8 interferes with AL fusion thus preventing downstream autophagosomal processing, whereas the overexpression of Plac8 can promote autophagic flux. Furthermore, activation of Rab7-dependent AL fusion bypasses the dependence on Plac8 suggesting that Plac8 functions in parallel to Rab7.

Upstream Activation of Autophagy Can Compensate for Plac8 Knockdown

In order to understand the relationship between Plac8 and autophagy activation, we tested the capacity of upstream

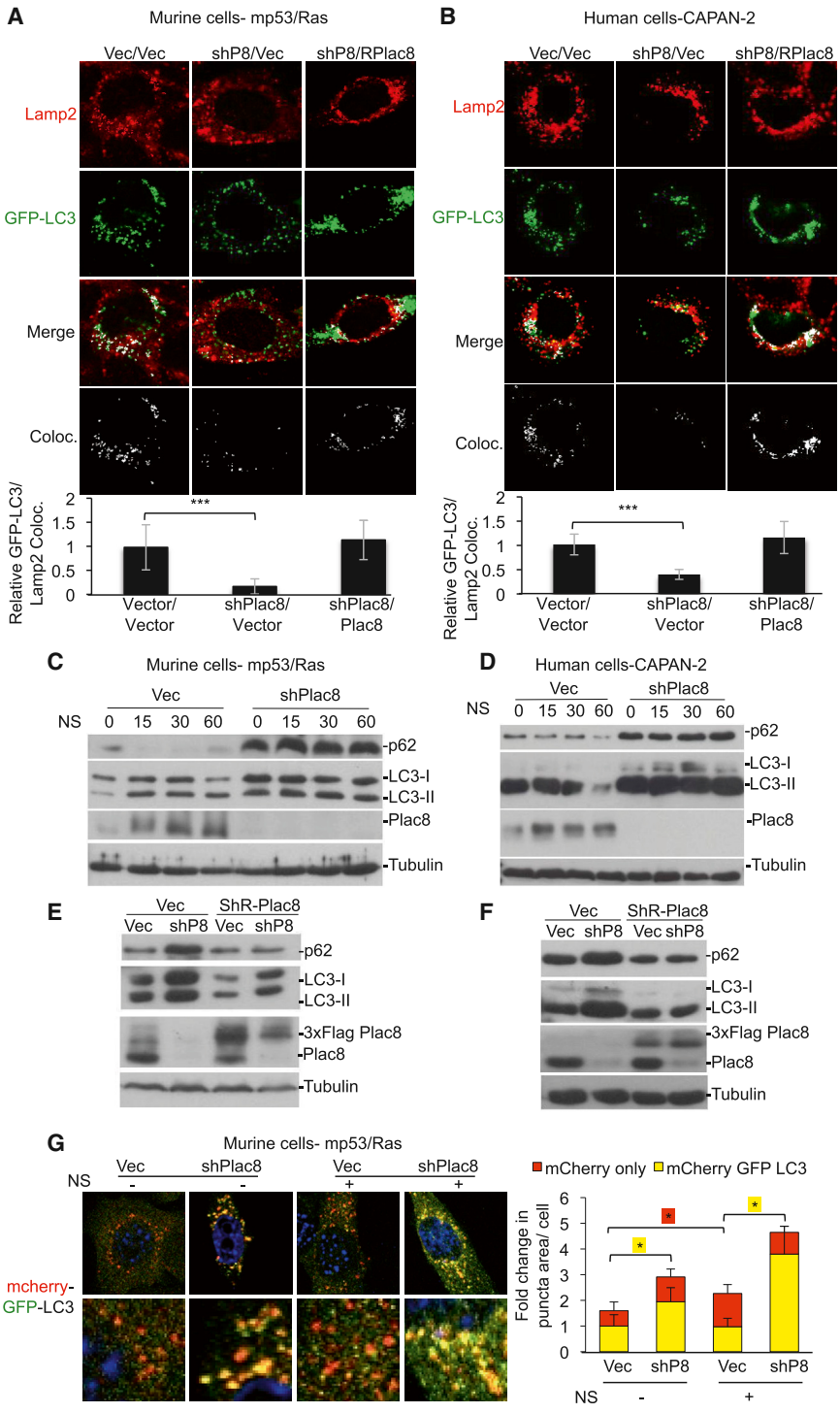

Figure 2. *Plac8* KD Results in the Accumulation of Autophagosomes and Autophagy Markers by Inhibiting Autophagosome-Lysosome Fusion

(A and B) (A) Murine mp53/Ras transformed and (B) human CAPAN-2 cells expressing GFP-LC3 and *Plac8* shRNA or *Plac8* shRNA with exogenous shRNA resistant Plac8 were nutrient starved in HBSS for 15 min, fixed, and stained for Lamp2. Fluorescence quantified by ImageJ. Relative ratios of autophagosomes fused with lysosomes per total autophagosomes are shown (±SD, ***$p < 0.001$, determined by Student's t test; $n \geq 50$ cells per cell line).

(C–F) Vector control (Vec) or Plac8 shRNA expressing mp53/Ras (C) and CAPAN-2 cells (D) were nutrient starved and immunoblotted for p62, LC3, and Plac8 (β-tubulin loading control). Lysates of mp53/Ras (E) and CAPAN-2 cells (F) expressing Vec, *Plac8* shRNA, exogenous 3 × Flag-tagged, shRNA-resistant *Plac8*, or *Plac8* shRNA with exogenous 3 × Flag-tagged, shRNA-resistant *Plac8* were immunoblotted for p62, LC3, Rab7, and Plac8.

(G) mp53/Ras cells expressing mCherry-EGFP-LC3 and Vec or *Plac8* shRNA were nutrient starved (NS) in HBSS or left untreated, fixed, and imaged via confocal microscopy. Representative images show a merge of red and green channels (yellow represents colocalization, i.e., autophagosomes; red indicates autolysosomes). Fluorescence intensities quantified by ImageJ. Fold changes in punctae area/cell are indicated (mean ± SD, Student's t test: *$p < 0.05$; $n \geq 100$ cells/cell line).

autophagy activation to compensate for Plac8 loss and diminished rates of AL fusion. We found that ectopic expression of Atg12, a ubiquitin-like protein covalently linked to Atg5 that forms a complex essential to autophagosome formation (Mizushima et al., 1998, 2001; Ohsumi, 2001), restored tumor formation capacity to Plac8 KD cells and increased AL fusion in these cells (Figures 5A–5D). Notably, in cells expressing ectopic Atg12 in the presence of Plac8 KD, p62, and LC3-II abundance is restored to levels found in unperturbed cells (Figures 5A and 5B), reflective of an autophagy rate restored to levels observed in the native cancer cells. In contrast, exogenous Atg12 expression in the absence of Plac8 KD was tumor inhibitory (Figures 5A and 5B), possibly due to proapoptotic functions (Rubinstein et al., 2011) or through hyperactivation of autophagy to levels inconsistent with survival. The reduction in steady-state levels of p62 and the increased ratio of LC3-II/LC3-I protein in cells expressing ectopic Atg12 support this latter hypothesis. Thus, whereas impaired AL fusion caused by Plac8 KD impedes PDA growth, upstream activation of the pathway can compensate for this. Moreover, consistent with an essential role of autophagy for the cancer phenotype, Atg12 KD inhibited tumor formation together with a decreased ratio of LC3-II/ LC3-I and p62 accumulation (Tanida et al., 2002) in both mp53/Ras and CAPAN-2 cells (Figure S5).

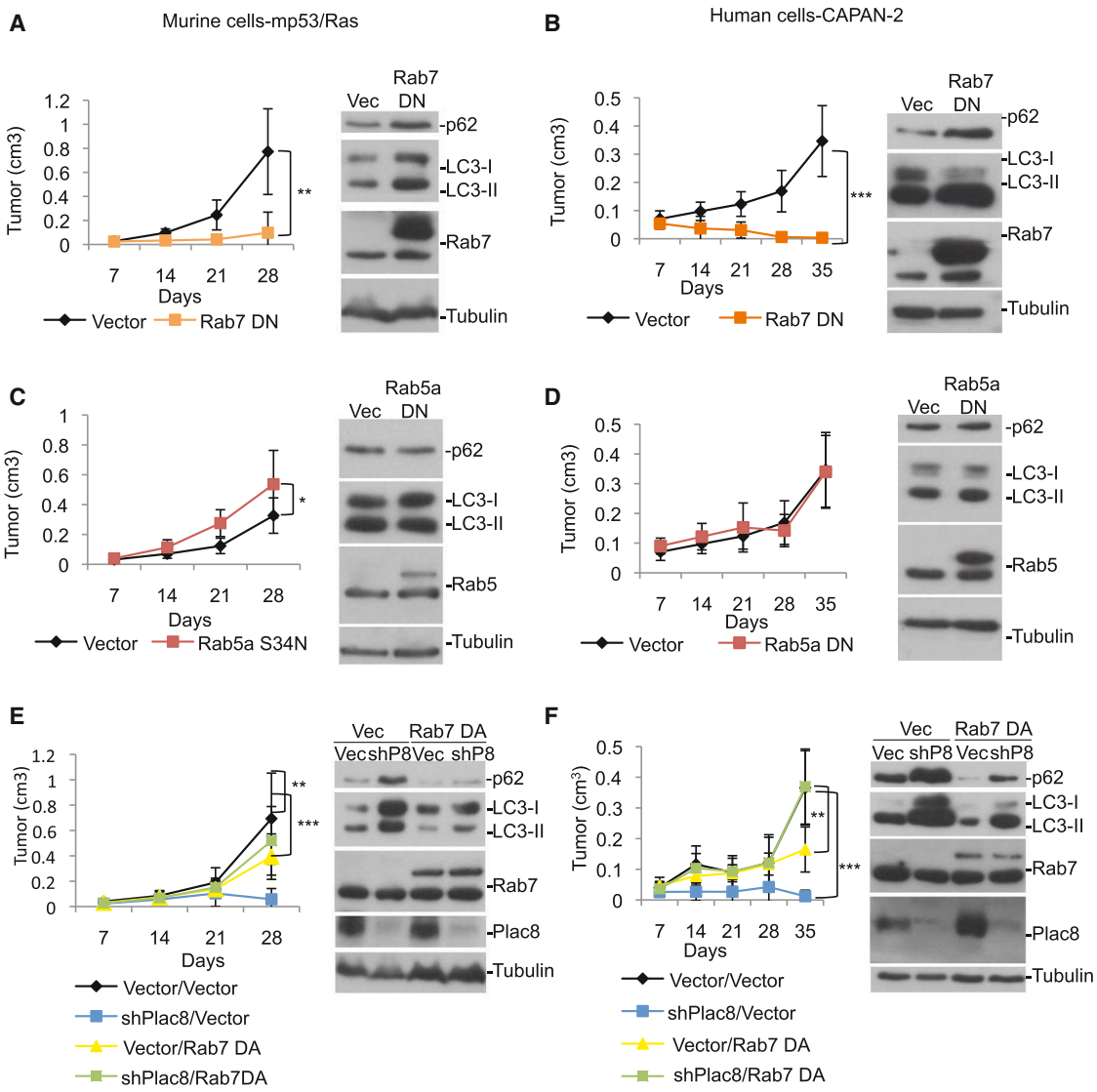

Figure 3. Activated Rab7 Rescues Cancer Phenotype in Plac8 KD Cells

Murine mp53/Ras cells (A, C, and E) and human CAPAN-2 cells (B, D, and F) were grafted into CD-1 nude mice, and tumor growth was monitored. Mean values of tumor volume ± SD and Student's t test at final time point are indicated (***p < 0.001; **p < 0.01; *p < 0.05; n ≥ 9 tumors per condition). Cells expressing 3 × Flag-tagged *Rab7* DN (Rab7T22N) or vector control (Vec) (A&B), 3 × Flag-tagged *Rab5a* DN (*Rab5aS34N*) or Vec (C&D), and 3 × Flag-tagged *Rab7* DA, *Plac8* shRNA, *Plac8* shRNA with 3 × Flag-tagged *Rab7* DA or Vec (E and F) were used. Corresponding cell lysates were immunoblotted for p62, LC3, Rab5 or Rab7 (A–F), and Plac8 in E&F (β-tubulin loading control).

Increased expression of Plac8 was noted in mp53/Ras cells in response to ectopic Rab7DA or ATG12 expression (Figures 3E, 3F, 5A, and 5B). This may occur as a response to stress, or as part of the program stimulating autophagy, considering Plac8 is able to stimulate autophagic flux in the presence of activated Ras (Figure S3).

Synergistic Induction of Autophagy by Activated *Ras* and Mutant *p53*

Mutations in both *KRAS* and *p53* have been linked with alterations in autophagy; however, their combined impact and the associated mechanisms are unknown (Guo et al., 2011; Livesey et al., 2012; Lock et al., 2011; Morselli et al., 2011; Tasdemir et al., 2008; Yang et al., 2011). Given the identification of Plac8 as a gene cooperatively upregulated by these mutations and its role in promoting AL fusion, we asked if autophagy rates would be regulated similarly by concurrent oncogenic mutations. To test this possibility, we compared accumulation of LC3 punctae following chloroquine treatment in YAMC cells, mp53, Ras, and mp53/Ras cells using the mCherry-EGFP-LC3 reporter. Notably, a significant increase in punctae was detected only in mp53/Ras cells, indicating that autophagic flux is induced synergistically by mutant *p53* and activated *Ras* (Figure 6).

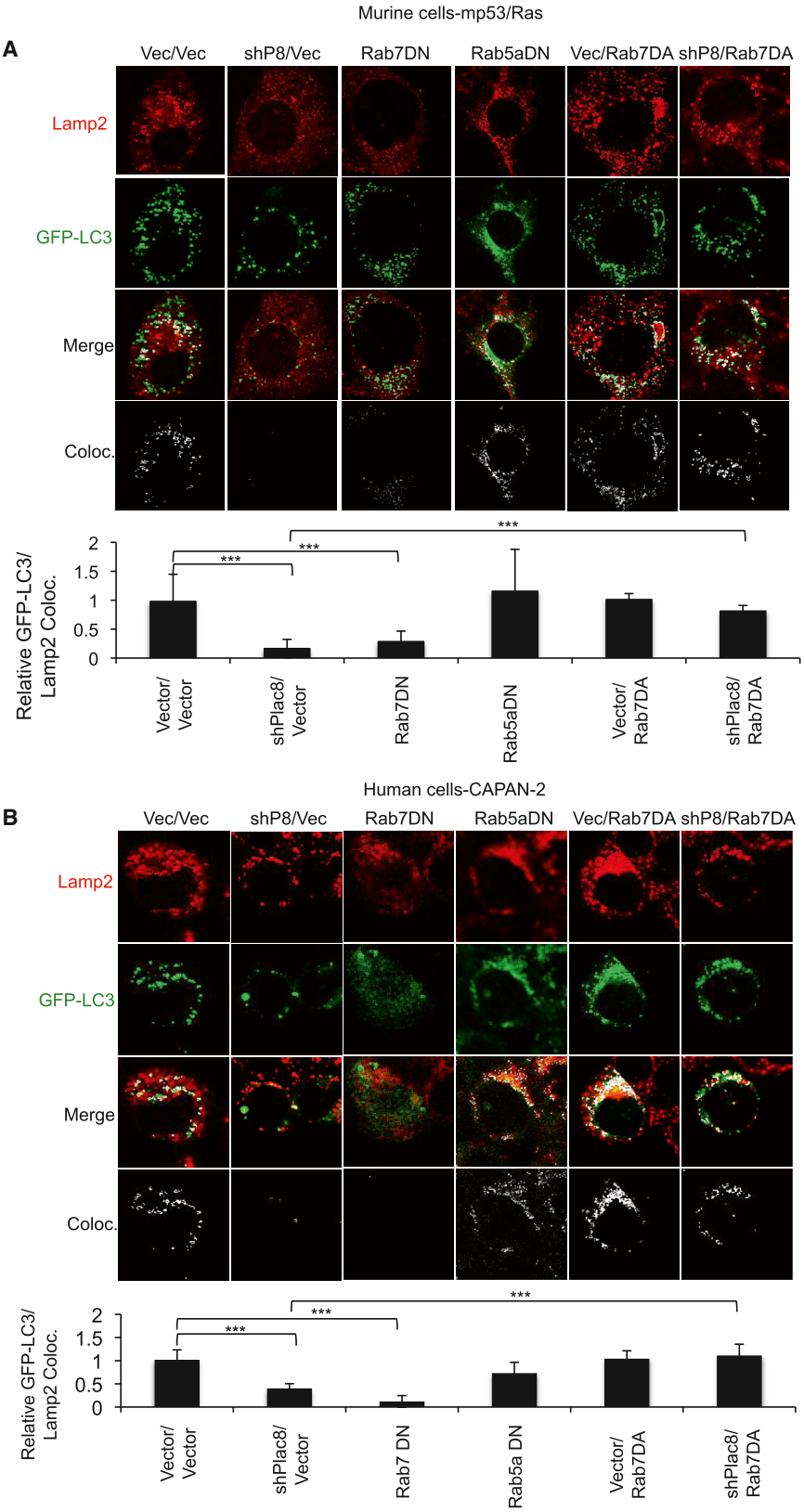

Figure 4. Activated Rab7 Rescues Autophagosome-Lysosome Fusion in Plac8 KD Cells

Murine GFP-LC3-mp53/Ras cells (A) and human GFP-LC3-CAPAN-2 cells (B) expressing vector control, Plac8 shRNA, 3 × Flag-tagged *Rab7* DN, 3 × Flag-tagged *Rab5a* DN, 3 × Flag-tagged *Rab7* DA, or *Plac8* shRNA and 3 × Flag-tagged Rab7DA were nutrient starved in HBSS for 15 min, fixed, stained for Lamp2, and imaged via confocal microscopy. Colocalization was determined and quantified by ImageJ. The ratios of autophagosomes fused with lysosomes (colocalized signal)/ total autophagosomes are indicated (mean ± SD; Student's t test; ***$p < 0.001$; $n \geq 50$ cells/cell line).

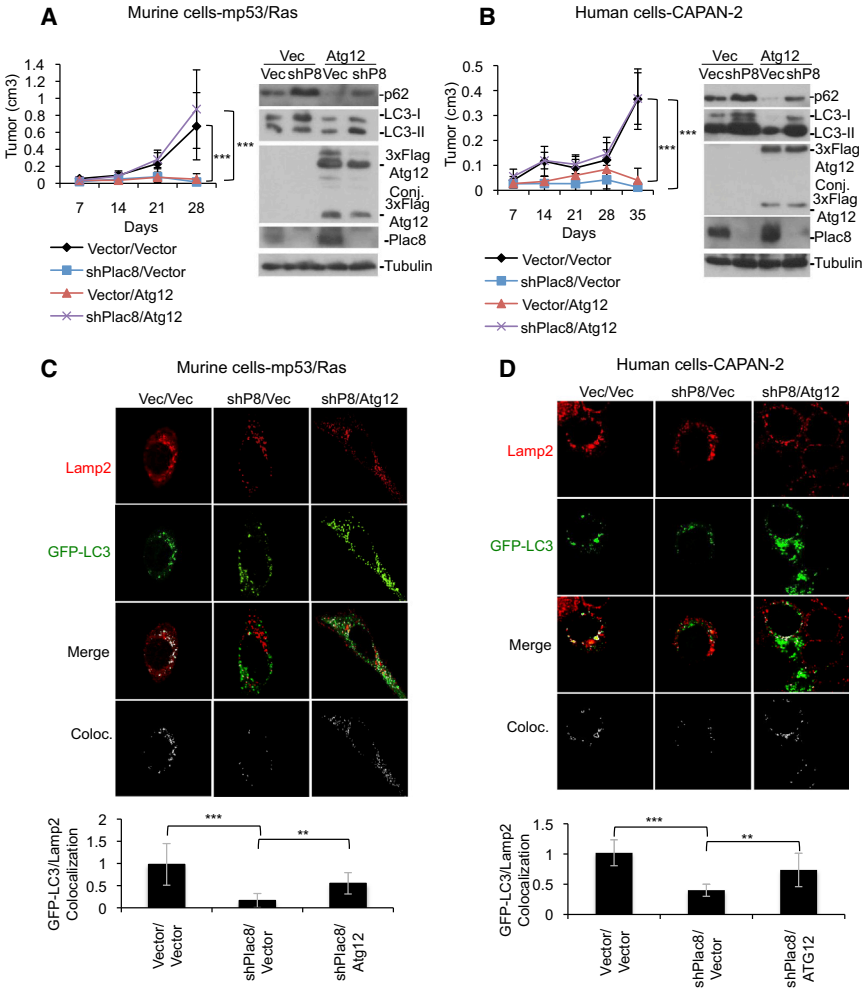

Figure 5. Overexpression of Atg12 Rescues Plac8 KD Inhibition of Cancer Phenotype and Autophagosome-Lysosome Fusion

Murine mp53/Ras cells (A) and human CAPAN-2 cells (B) were grafted into CD-1 nude mice and tumor growth was monitored. Mean values of tumor volume ±SD and Student's t test at final time point are indicated (***$p < 0.001$; $n \geq 9$ tumors per condition). Cells expressing vector control (Vec), 3 × Flag-tagged *Atg12*, *Plac8* shRNA, or *Plac8* shRNA and 3 × Flag-tagged *Atg12* were used. Corresponding cell lysates were immunoblotted for p62, LC3, Atg12, and Plac8. GFP-LC3-mp53/Ras cells (C) and GFP-LC3-CAPAN-2 cells (D) expressing Vec, Plac8 shRNA, or Plac8 shRNA and 3 × Flag-tagged Atg12 were nutrient starved in HBSS for 15 min fixed, stained for Lamp2, and imaged via confocal microscopy. Colocalization was determined and quantified by ImageJ. The ratios of autophagosomes fused with lysosomes (colocalized signal)/total autophagosomes are indicated (mean ± SD; Student's t test ***$p < 0.001$; **$p < 0.01$; $n \geq 50$ cells/line).

Plac8 Depletion Does Not Alter Lysosomal pH

Inhibitors of AL fusion such as bafilomycin A1 or CQ act via disrupting lysosomal pH (Klionsky et al., 2012; Yamamoto et al., 1998). Plac8 KD, however, had no effect on lysosomal pH (Figure S6A). Consistent with this finding lysosomal pH-dependent endocytic degradation of epidermal growth factor receptors (EGFRs) (Ganley et al., 2011) was unaffected by Plac8 KD (Figure S6B). Similarly, Plac8 KD has no detectable effect on endocytosis, as visualized by cellular dextran uptake (Figure S6C). Taken together, our data suggest that Plac8 functions via mechanisms that modulate rates of AL fusion without affecting lysosomal pH or endocytic degradation.

Inhibition of autophagosome-lysosome fusion by CQ has also been associated with an increase in cellular reactive oxygen species (ROS) suggesting a role for autophagy in coping with oxidative stress (Yang et al., 2011). Although we found CQ-mediated increases of ROS levels in mp53/Ras cells, Plac8 KD had no impact on cellular ROS, as detectable by DCF staining (Figures S6D and S6E), suggesting that inhibition of autophagosome-lysosome fusion is not necessarily associated with increases in cellular ROS. Conversely, induction of cellular ROS following CQ exposure thus may be unrelated to modulation of autophagic flux.

Mutation of *Plac8* Extends Survival in a Kras-p53 PDA-Engineered Mouse Model

To extend our findings in xenograft models, we evaluated the importance of Plac8 in PDA progression and biology using a Pdx1-Cre; LSL-$Kras^{G12D}$; $p53^{L/+}$ genetically engineered mouse PDA model. This model exhibits successive stages of cancer progression (referred to as pancreatic intraepithelial neoplasia or PanIN I–III) leading to PDA, that typifies the human disease. Tumor progression is associated with loss of the wild-type *p53* allele, and thus all ensuing tumors are *p53* null (Bardeesy et al., 2006a). Cohorts of Pdx1-Cre; LSL-$Kras^{G12D}$; $p53^{L/+}$ mice with concurrent germline $Plac8^{+/+}$, or $Plac8^{-/-}$ mutations, henceforth referred to as PDA-$Plac8^{wt}$ and PDA-$Plac8^{null}$ were created using established strains (Bardeesy et al., 2006a; Ledford et al., 2007). Mice were born at expected Mendelian ratios and were indistinguishable from each other with regards to outward appearance and activity through the first 8 weeks of life as expected (Ledford et al., 2007). Individuals were followed longitudinally until signs of illness necessitated necropsy (see Experimental Procedures). Overall survival of the PDA-$Plac8^{null}$ cohort (OS 27.9 weeks) was significantly longer than the PDA-$Plac8^{wt}$ cohort (OS 17.0 weeks, $p = 0.0006$) (Figure 7A) demonstrating in vivo that genetic inactivation of *Plac8* impedes cancer progression and resulting death. Thus, Plac8 has a central role in PDA pathogenesis.

The increased survival of the PDA-$Plac8^{null}$ cohort could be due to an impact on tumor progression in the early stages of tumor initiation, namely, the formation of PanIN precursor lesions, or in the later stages of fully advanced PDA growth. To differentiate these possibilities, we conducted a histological survey of the pancreas of PDA-$Plac8^{null}$ and PDA-$Plac8^{wt}$ at 9 weeks of

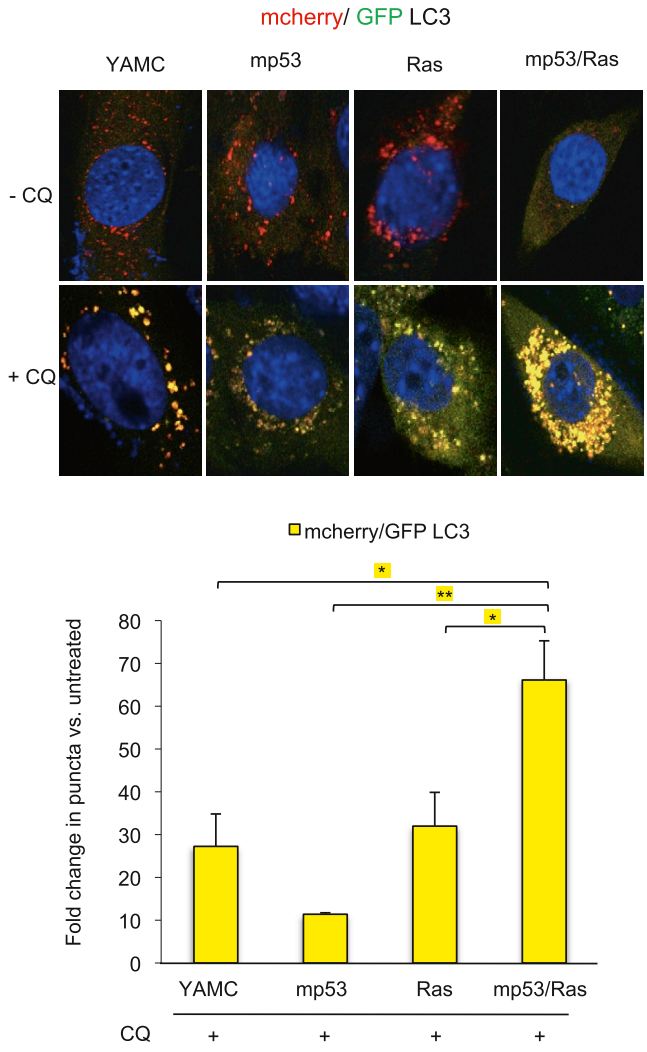

Figure 6. Synergistic Induction of Autophagic Flux by Mutant p53 and Activated Ras

YAMC, mp53, Ras, and mp53/Ras cells expressing mCherry-EGFP-LC3 were exposed to 25 μM chloroquine (CQ) for 24 hr or left untreated, fixed, and imaged using confocal microscopy. Representative images show the merge of red and green channels, with yellow representing signal colocalization. Autophagosomes (yellow) and autolysosomes (red) quantified using ImageJ. Fold changes in punctae areas/cell are indicated (mean ± SD; Student's t test; $^{**}p < 0.01$; $^{*}p < 0.05$; $n \geq 50$ cells/line).

age just prior to the onset of lethal advanced tumors. Quantification of normal ducts, as well as, early and late PanIN revealed no significant differences in the prevalence of premalignant lesions between the groups (Figures 7B and S7). Therefore, Plac8 loss has minimal effect on the early stages of tumor initiation, indicating that Plac8 rather contributes to the progression of advanced PanINs and PDA.

To gain further insight into the relationship between Plac8, autophagy control, and PDA pathogenesis, we crossed a GFP-LC3 transgenic strain with our Kras-p53 model, enabling us to measure autophagy in vivo (Kuma et al., 2004). In this model (GFP-LC3; Pdx1-Cre; LSL-$Kras^{G12D}$; $p53^{L/+}$), in which the wild-type *p53* allele is lost during the course of PanIN progression toward cancer (Bardeesy et al., 2006a), we found an increase in LC3 punctae, indicating increased numbers of epithelial autophagosomes, with each successive histological stage of cancer progression, with highest levels in PDA, and virtually no punctae in normal ducts or low grade PanIN-1 (Figure 7C). Consistent with this finding, immunofluorescent staining of histological sections indicated Plac8 expression in PanINs and PDA, whereas Plac8 staining is not detectable in normal pancreatic ducts. In addition, Plac8 staining colocalizes with Lamp2 staining, confirming lysosomal localization of Plac8 in PDA (Figures 7D and 7E) Taken together, the marked and specific activation of autophagy in advanced PDA matches well with the specific impact of *Plac8* inactivation on the later stages of disease.

DISCUSSION

Synergistic regulation downstream of cooperating oncogenic mutations has emerged as a reliable indicator of genes critical to malignant cell transformation in a variety of contexts including cancer-initiating cells (McMurray et al., 2008; Ashton et al., 2012). Here, we identify such a gene, *Plac8*, as a regulator of autophagosome-lysosome fusion required for PDA growth, thus providing a mechanistic link between oncogenic mutations and the activation of autophagy in cancer. Activated by oncogenic *KRAS* and *p53* loss of function, two of the most commonly occurring mutations in cancer, Plac8 expression is required for growth of human pancreatic cancer cells as xenografts in mice, as well as activation of autophagy in vitro and in vivo where we observe that both *RAS* and *p53* mutations are critical for elevated autophagy rates. Our data also suggest that the role of Plac8 in facilitating autophagy is critical to the cancer phenotype, as the requirement of Plac8 for both tumorigenicity and autophagy can be compensated by overexpression of Atg12, a gene critical for autophagosome formation (Mizushima et al., 1998), or by constitutively activated *Rab7*, a gene encoding a GTP-binding protein stimulating autophagosome-lysosome fusion (Gutierrez et al., 2004; Jäger et al., 2004). This is consistent with an interpretation that tumor growth of *Plac8*-deficient cells is compromised due to suboptimal autophagic flux. Notably, we also show that Plac8 may offer a potential therapeutic window and point of intervention, as *Plac8* germline mutation in an engineered PDA model inhibits cancer progression and significantly improves survival while having a minimal impact on the overall fitness of the animals. This suggests that *Plac8*, and regulation of autophagosome-lysosome fusion, has specific relevance to regulation of autophagy during malignant cell transformation. Independent support for the oncogenic potential of the *Plac8* gene comes from several in vivo genetic screens in which *Plac8* has been identified repeatedly as a target for retroviral insertion mutagenesis, implicating its deregulation as a driving force in carcinogenesis (Kool et al., 2010; Williams et al., 2006).

Plac8 is a lysosomal protein that facilitates autophagosome-lysosome fusion without affecting endocytic protein degradation and lysosomal pH. This is in contrast to Rab7 and SNARE proteins, such as VAMP8, that impact both autophagosome-lysosome fusion and endocytic protein degradation (Furuta et al.,

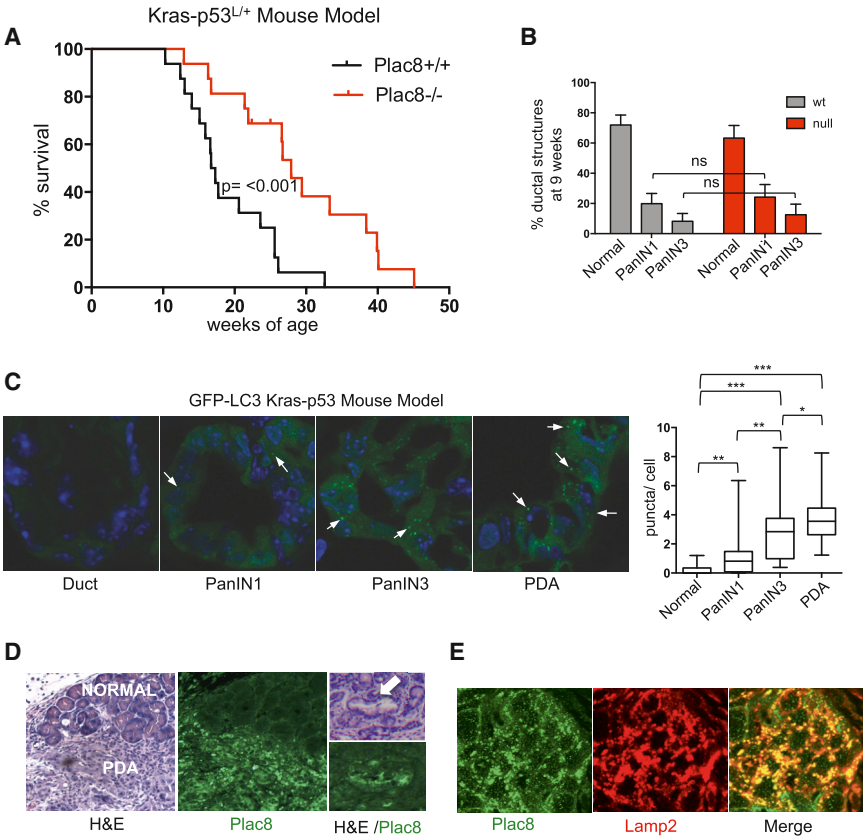

Figure 7. *Plac8* Mutation Impedes Advanced Tumor Progression in the Kras-p53 Mouse PDA Model

(A) Kaplan-Meier analysis of cohorts of Pdx1-Cre;LSL-*Kras*^{G12D};*p53*$^{L/+}$ mice with concurrent germline *Plac8*$^{+/+}$ or *Plac8*$^{-/-}$ mutations. Overall survival is increased in Plac8^{null} cohort (27.9 weeks) compared with Plac8^{wt} (OS 17. weeks, p = 0.0006).

(B) Whole pancreatic histological analysis of Pdx1-Cre;*LSL-Kras*^{G12D};*p53*$^{L/+}$ mice with concurrent germline Plac8$^{-/-}$ mutations (n = 6) versus Plac8 WT (n = 10) at 9 weeks of age demonstrated similar burdens of PanIN. Data are presented as a fraction of the total with confidence intervals. Three of ten wild-type compared to 0/6 Plac8$^{-/-}$ harbored advanced PDA.

(C) Epithelial cell GFP punctae (white arrows) harbored within normal ducts, pancreatic intraepithelial neoplasia I and III (PanIN I&III), and PDA (n = 50 cells/lesion) were quantified from cohort of Pdx1-Cre; LSL-Kras^{G12D};p53$^{L/+}$;GFP-LC3 mice (n = 6 mice; significance determined by the Mann-Whitney test ***p < 0.001; **p < 0.01; *p < 0.05).

(D) Immunoflourescent staining of Plac8 in normal pancreatic duct, PanIN (white arrow) and PDA from Pdx1-Cre; LSL-Kras^{G12D};p53$^{L/+}$ mice. Adjacent H&E-stained sections were evaluated to determine histologic classification.

(E) PDA tissue from Pdx1-Cre;LSL-Kras^{G12D};p53$^{L/+}$ stained with Plac8 and Lamp2 antibodies, visualized with Alexa 488 (green) and Alexa 555 (red), respectively.

2010; Gutierrez et al., 2004; Klionsky et al., 2012; Wong et al., 1998). The apparently minimal impact of *Plac8* deficiency on normal physiologic processes (Ledford et al., 2007) fits well with the mutant phenotypes of several other genes involved in the autophagosome maturation including *Lamp2* and *Tecpr1* (Chen et al., 2012; Eskelinen et al., 2002; Ogawa et al., 2011; Tanaka et al., 2000). Unlike many *Atg*-family mutant mice, which are not viable (Komatsu et al., 2005; Kuma et al., 2004), *Plac8*, *Lamp2*, and *Tecpr1* mutant mice can all survive through adulthood, though all suffer from a diminished capacity to clear infections, due to defects in lysosomal function (Beertsen et al., 2008; Binker et al., 2007; Ledford et al., 2007; Ogawa et al., 2011). Thus, later stages of autophagy and autophagosome maturation may provide a variety of attractive therapeutic opportunities where inhibition of steps in this process are likely better tolerated by normal tissues but not by tumors that depend on a high autophagic rate.

Plac8 was identified originally as a leukocyte inhibitory factor regulated gene in the mouse uterus and also in genome-wide expression analysis of the placenta, from where its name is derived (Galaviz-Hernandez et al., 2003). It has been functionally ascribed to the regulation of a number of distinct cellular processes (Rogulski et al., 2005; Wu et al., 2010). *Plac8* knockout mice have been found to suffer increased adiposity at advanced ages leading to the discovery of a role in brown fat differentiation through induction of C/EBPbeta expression (Jimenez-Preitner et al., 2011). Of note, we did not find significant differences in levels of C/EBPbeta expression among PDA cell lines with or without *Plac8*. Because our data point toward an extranuclear location in epithelial cells, within the lysosomal compartment where it facilitates autophagosome-lysosome fusion, it seems plausible that *Plac8* may have differing roles among different cell types.

Here, we find that concurrent mutation of *KRAS* and *p53* is critical for maximal induction of autophagy, and correspondingly, we see a stepwise incremental increase in LC3 puncta in vivo with each histological stage through the course of PDA progression. Thus, we find that the cooperative effects of *KRAS* and *p53* drive activation of autophagy rather than either mutation alone. This is consistent with established associations between autophagy dependence and *RAS* mutant tumor cell lines, many of which harbor *p53* mutations (Guo et al., 2011; Lock et al., 2011; O'Dell et al., 2012; Yang et al., 2011). Others have reported conflicting roles of p53 in regulating autophagy (Morselli et al., 2011; Tasdemir et al., 2008), with a recent report showing that in a setting of homozygous p53 deletion during embryonal development loss of autophagy accelerates pancreatic tumor progression (Rosenfeldt et al., 2013). We elected to study autophagy in vivo using a model in which loss of p53 function occurs in a stepwise progressive manner relying on the spontaneous loss of a heterozygous WT p53 allele (Bardeesy et al., 2006a) as a late mutational event mimicking human PDA progression (Hruban et al., 2001; Lüttges et al., 2001). In this context, we observe full autophagy activation at later stages of

tumor formation. Correspondingly, it is at this point in advanced PanIN and PDA, when autophagy is most active, that we observe a delay in tumor progression in the absence of Plac8. In contrast, we do not see any effect of loss of *Plac8* in a PDA model in which both copies of the conditional *p53* allele are somatically mutated during embryogenesis (Figure S8), suggesting that the timing of complete p53 loss in the natural history and progression of PDA impacts the resulting tumor's dependencies.

Pancreatic ductal adenocarcinoma (PDA) remains a significant challenge clinically despite iteration of many of the pathways and processes downstream of the signature genetic lesions (Hezel et al., 2006; Hidalgo, 2010). Further highlighting this is the fact that the most significant treatment advance in the past decade has come from a new combination of traditional chemotherapies rather than any particular novel genetic or biologic revelation (Conroy et al., 2011). Although insights into improving drug delivery, modulation of the tumor microenvironment, and additional downstream effectors of *KRAS* have recently pointed to alternative therapeutic strategies, new processes and targets critical to PDA growth are needed (DeNicola et al., 2011; Frese et al., 2012; Olive et al., 2009; Provenzano et al., 2012; Rhim et al., 2012). Although pharmacologic inhibition of autophagy is under ongoing evaluation clinically, there are limited agents available; moreover, autophagy plays a critical role in normal tissue homeostasis and energy balance making the identification of a therapeutic window potentially difficult. Thus, regulators and effectors of autophagy specific to tumors, such as *Plac8*, could potentially offer valuable targets for intervention.

EXPERIMENTAL PROCEDURES

Cells

YAMC, mp53, Ras, mp53/Ras cell derivation and maintenance were described previously (McMurray et al., 2008; Xia and Land, 2007). CAPAN-2, PANC-1, and Panc10.05 cell lines were obtained from ATCC.

Antibodies and Compounds

The following antibodies were used: rabbit polyclonal antibody raised against the c-terminal 16 amino acids of murine Plac8 (Ledford et al., 2007) (Pocono Rabbit Farm & Laboratories), rabbit polyclonal anti-β-Tubulin antibody (H-235, Santa Cruz Biotechnology), rat monoclonal anti-Lamp2 antibody (GL2A7, Abcam), mouse monoclonal anti-Rab7 antibody (R8779, Sigma), rabbit polyclonal anti-LC3B antibody (L7543, Sigma), mouse monoclonal anti-RhoA antibody (sc-418, Santa Cruz), goat polyclonal anti-cathepsin D antibody (sc-6486, Santa Cruz), guinea pig polyclonal anti-p62 antibody (GP62-C, PROGEN), mouse monoclonal anti-3 × Flag antibody and HRP-conjugated anti-3 × Flag antibody (F2426 and A8592, Sigma), rabbit polyclonal anti-Rab5 antibody (ab18211, Abcam), rabbit polyclonal anti-Atg12 antibody (A8731, Sigma), and EGFR antibody (sc 03).

The following compounds were used: bafilomycin A1 (Sigma B1793), chloroquine (Sigma 6628), and cycloheximide (Sigma C7698, Lysosensor Yellow Blue DND-160 and DCF-DA (Molecular Probes, L-7545 and C6827, respectively).

Plasmids

Plasmids for retroviral Plac8 KD and shRNA-resistant Plac8 expression were described previously (McMurray et al., 2008). cDNAs for Rab7, Rab5a, and Atg12 were PCR cloned in pBabe-hygro containing an in-frame, N-terminal 3 × Flag tag and sequence verified. Dominant-negative and activated Rab7 and Rab5a mutants were generated via site-directed mutagenesis and sequence verified. N-terminal 3 × Flag-tagged DN Rab7, DA Rab7, DN Rab5a, and Atg12 were PCR cloned in pLenti/Ubc/V5 (Invitrogen) and sequence verified. cDNA for LC3 was PCR cloned in pEGFP (Clontech Laboratories) and subsequently PCR cloned into lentiviral vector FG12. The mCherry-EGFP-LC3 puro construct (Addgene 22418) (N'Diaye et al., 2009) was cloned into pBabe-hygro. Atg12 shRNA molecules were designed (http://jura.wi.mit.edu/bioc/siRNAext/home.php) and cloned into the pSuper-retro system (Oligoengine). Atg12 lentiviral KD constructs were obtained from Openbiosystems.

Immunofluorescent Staining of Cells

Cells were plated onto collagen-1-coated 22 mm glass coverslips (BD Biosciences). Cells were fixed and incubated with primary antibody overnight at 4°C while shaking followed by appropriate secondary antibodies. Immunostained cells were (1) washed three times for 10 min with PBS, (2) mounted in VectaShield Mounting Media (Vector Laboratories), and (3) analyzed and imaged using a SP5 Leica inverted confocal microscope.

Subcellular Fractionation and Lysosome Isolation

mp53/Ras cells were grown for 2 days at 39°C in RPMI with 10% (v/v) FBS, before pelleting at 1,200 rpm for 5 min at 4°C. A fraction was retained and lysed in RIPA buffer for the whole-cell lysate (WC) sample. Lysosomes were then isolated using a Lysosomal Isolation Kit (Sigma). In short, the cell pellet was resuspended, then homogenized in a Dounce homogenizer, and centrifuged at 1,000 × *g* for 10 min. The pellet was saved as the nuclear fraction (N) sample. The supernatant was then centrifuged at 20,000 × *g* for 20 min, and supernatant was removed and saved as the cystosolic fraction (C). The pellet was resuspended in a small aliquot as the crude lysosomal fraction (CL). To separate lysosomes from other organelles 505 μl of Optiprep and 275 μl of Optiprep dilution buffer were added per 800 μl of resuspended crude lysosomal fraction. $CaCl_2$ was added to final concentration of 8 mM, followed by 15 min incubation on ice and centrifugation at 5000 × *g* for 10 min at 4°C. Purified lysosomal fraction (L) (supernatant) and microsomal pellet (M) were retained. Pellets were resuspended in RIPA; protein was determined by Bradford assay. SDS sample buffer was added to all samples.

Proteinase K Treatment of Lysosomes

The crude lysosomal fraction was isolated as described above and resuspended in 50 mM Tris buffer (pH 7.4). Crude lysosomal fractions were divided and treated for 30 min at 37°C with (1) buffer, (2) 0.5 μg/ml PK, (3) 0.5 μg/ml PK + 1.0% Triton X-100. Samples were then placed on ice, PK activity was quenched with 1 mM phenylmethanesulfonylfluoride, and SDS sample buffer was added.

Xenograft Assays

Matrigel (BD Biosciences) was mixed with PANC-1 and Panc10.05 cell/medium mixture in a 1:1 ratio. Cell mixtures were then injected bilaterally into the flanks of CD-1 nude mice (Crl:CD-1-Foxn^{nu}, Charles River Laboratories) in the following cell numbers: mp53/Ras, 5 × 10^5 cells, and CAPAN-2, 5 × 10^5 cells. Cell mixtures were injected into the flanks of NOD/SCID mice (Charles River Laboratories) in the following cell numbers per injection: PANC-1, 2.5 × 10^6 cells, and Panc10.05, 1 × 10^6 cells. Tumor size was measured every 7 days by caliper and volume calculated by the formula volume = $(4/3)\Pi r^3$, using the average of two orthogonal radius measurements; significance of difference in tumor size was calculated by t test.

Quantification of GFP-LC3 and mCherry-EGFP-LC3 Punctae, and of Lamp2/GFP-LC3 Colocalization

Cells were fixed, stained, mounted, and imaged by the methods described above. GFP-LC3 punctae were determined using the ImageJ plug-in Watershed Segmentation. The image produced by selecting Object/Background binary was inverted and overlayed on top of the GFP-LC3 image. The resulting image was quantified by measuring the mean green and blue signals per image and dividing the blue signal by the total green signal to get the amount of punctae per total GFP-LC3 expressed in the cell and then normalized to the mean YAMC ratio of punctae formation. To quantify GFP-LC3 colocalization, the ImageJ plug-in Co-localization Finder was used to determine colocalization (in white) of red (Lamp2) and green (GFP-LC3) signal. The mean colocalized

signal were then divided by the GFP-LC3 signal to derive a ratio of colocalization per GFP-LC3 signal, and these ratios were then normalized to the mean values derived from vector control or YAMC cells. The mCherry-EGFP-LC3 reporter was used to determine ratios of autophagosomes (red and green colocalized signal) and autolysosomes (red signal only). The Red and Green Punctae Co-localization plug-in in ImageJ was used to derive the puncta areas per cell. The area value for autolysosomes was determined by subtracting the red and green colocalized signal from the red puncta area and normalized to the mean of the mCherry-EGFP-LC3 puncta area of vector control or untreated control samples.

Mice

Mutant Mouse Strains

All animal studies were conducted in accordance with the AAALAC accredited University Committee on Animal Resources (UCAR). All mouse strains used in these studies have been previously described and characterized (Bardeesy et al., 2006a; Kuma et al., 2004; Ledford et al., 2007). Specifically $Kras^{G12D}$, $p53^{L/L}$, $Plac8^{-/-}$, GFP-LC3, and Pdx-Cre mutant strains were intercrossed to achieve the desired cohorts as outlined above. The genetic background was mixed. Individual mice within experimental cohorts were followed until signs of illness including poor grooming, abdominal bloating, diminished activity, or weight loss at which point a full necropsy was performed followed by histological analysis.

Histology and In Vivo GFP-LC3- Analysis

A board-certified pathologist with a specialization in pancreatic histopathology independently reviewed and classified tumors. Lymph nodes, lungs, and spleen were included in a survey for metastasis in all individuals with tumors. To determine the extent of PanIN formation at 9 weeks of age, the whole pancreas from wild-type and Plac8-null Kras-p53 PDA mice (n = 6–10/ group) was sectioned lengthwise. Ductal structures were analyzed using hematoxylin and eosin (H&E)-stained sections and classified as normal, PanIN1, or PanIN3. To determine formation of LC3 punctae, in vivo frozen sections from compound GFP-LC3 Kras-p53 mutant pancreas were analyzed as previously described by confocal microscopy (Kuma et al., 2004). Adjacent H&E-stained sections were evaluated by C.L.W.-M. to determine histologic classification (normal ducts, PanIn1 or 3, or PDA). In summary n = 3 mice encompassing each histologic type of lesion were evaluated. Punctae and nuclei from ductal structures (normal and PanIN1–3) and well-differentiated PDA (in which a distinction could be made histologically between tumor and stroma) were manually counted as well as determined by ImageJ. Because results between manual counts and those determined by ImageJ analysis were consistent, ImageJ analysis is presented.

Survival Analysis

Survival was determined using the Kaplan-Meier method, and comparisons between groups were determined using the log-rank test. All statistical analyses were performed using Prism statistical software version 4.0a May 11, 2003. Animals that displayed signs of illness and were found to have advanced cancers on necropsy were included as events as were all animals that died prior to developing signs of illness that had a pancreatic mass and histological diagnosis of adenocarcinoma identified at autopsy. Animals that died for reasons other than advanced cancer, as determined by the absences of pancreatic pathology on autopsy, were censored.

Immunofluorescent Staining of Tumor Sections

Whole pancreas from wild-type and Plac8-null Kras-p53 PDA mice was paraffin embedded and sectioned lengthwise. Slides were baked in a 60°C oven for 1 hr followed by routine deparafinization. Antigen retrieval was then performed in a pressure cooker with 1× Rodent decloaker (Biocare Medical). Slides were blocked with 3% hydrogen peroxide, rinsed well in phosphate buffered saline, and incubated with Plac8 antibody at 1:500 dilution at room temperature and then anti-rabbit Alexa 488 secondary antibody for 30 min at room temperature. The tissue sections were next incubated with the Lamp2 and anti-rat Alexa 555 secondary antibody sequentially as described above. The sections were rinsed again, dehydrated in 100% ethanol, mounted, and imaged using confocal microscopy.

SUPPLEMENTAL INFORMATION

Supplemental Information includes Supplemental Experimental Procedures and eight figures and can be found with this article online at http://dx.doi.org/10.1016/j.celrep.2014.03.061.

AUTHOR CONTRIBUTIONS

C.K. designed and performed genetic, biochemical, and colocalization analyses and the experiments shown in Figure S4. V.B. designed and performed autophagic flux experiments and their analysis, molecular tissue analyses, and the work shown in Figures S3 and S6. M.R.O. carried out breeding experiments and their analysis, J.L.H. carried out LC3 in vivo analysis, L.N. carried out molecular biology work, and C.L.W.-M. performed assessment of tissue sections. A.F.H. and H.L. directed and coordinated the project.

ACKNOWLEDGMENTS

We would like to thank Dr. Beverly H. Koller for *Plac8*^{null} mice, Karen Bentley for electron microscopy, Dr. Shanshan Pei for FACS analysis, Loralee McMahon for histology, Nicole Scott for advice, and Drs. Dirk Bohmann and Mark Noble for critical reading of the manuscript. This work has been supported by NIH grants CA90663, CA120317, and CA138249 to H.L. and CA122835 and CA172302 to A.F.H. A.F.H. has also been supported by an HHMI early career award, the Edelman-Gardner Cancer Research Foundation award, a University of Rochester Buswell Fellowship, and the generous support of the Pancreatic Cancer Association of Western New York and the Michael F. Contestabile Memorial Golf Tournament.

Received: April 5, 2013
Revised: February 12, 2014
Accepted: March 24, 2014
Published: May 1, 2014

REFERENCES

Aguirre, A.J., Bardeesy, N., Sinha, M., Lopez, L., Tuveson, D.A., Horner, J., Redston, M.S., and DePinho, R.A. (2003). Activated Kras and Ink4a/Arf deficiency cooperate to produce metastatic pancreatic ductal adenocarcinoma. Genes Dev. *17*, 3112–3126.

Ashton, J.M., Balys, M., Neering, S.J., Hassane, D.C., Cowley, G., Root, D.E., Miller, P.G., Ebert, B.L., McMurray, H.R., Land, H., and Jordan, C.T. (2012). Gene sets identified with oncogene cooperativity analysis regulate in vivo growth and survival of leukemia stem cells. Cell Stem Cell *11*, 359–372.

Balaburski, G.M., Hontz, R.D., and Murphy, M.E. (2010). p53 and ARF: unexpected players in autophagy. Trends Cell Biol. *20*, 363–369.

Bardeesy, N., Aguirre, A.J., Chu, G.C., Cheng, K.H., Lopez, L.V., Hezel, A.F., Feng, B., Brennan, C., Weissleder, R., Mahmood, U., et al. (2006a). Both p16(Ink4a) and the p19(Arf)-p53 pathway constrain progression of pancreatic adenocarcinoma in the mouse. Proc. Natl. Acad. Sci. USA *103*, 5947–5952.

Beertsen, W., Willenborg, M., Everts, V., Zirogianni, A., Podschun, R., Schröder, B., Eskelinen, E.L., and Saftig, P. (2008). Impaired phagosomal maturation in neutrophils leads to periodontitis in lysosomal-associated membrane protein-2 knockout mice. J. Immunol. *180*, 475–482.

Biankin, A.V., Waddell, N., Kassahn, K.S., Gingras, M.C., Muthuswamy, L.B., Johns, A.L., Miller, D.K., Wilson, P.J., Patch, A.M., Wu, J., et al.; Australian Pancreatic Cancer Genome Initiative (2012). Pancreatic cancer genomes reveal aberrations in axon guidance pathway genes. Nature *491*, 399–405.

Binker, M.G., Cosen-Binker, L.I., Terebiznik, M.R., Mallo, G.V., McCaw, S.E., Eskelinen, E.L., Willenborg, M., Brumell, J.H., Saftig, P., Grinstein, S., and Gray-Owen, S.D. (2007). Arrested maturation of Neisseria-containing phagosomes in the absence of the lysosome-associated membrane proteins, LAMP-1 and LAMP-2. Cell. Microbiol. *9*, 2153–2166.

Bucci, C., Parton, R.G., Mather, I.H., Stunnenberg, H., Simons, K., Hoflack, B., and Zerial, M. (1992). The small GTPase rab5 functions as a regulatory factor in the early endocytic pathway. Cell *70*, 715–728.

Buchholz, M., Braun, M., Heidenblut, A., Kestler, H.A., Klöppel, G., Schmiegel, W., Hahn, S.A., Lüttges, J., and Gress, T.M. (2005). Transcriptome analysis of microdissected pancreatic intraepithelial neoplastic lesions. Oncogene *24*, 6626–6636.

Chen, X., and Wang, Z. (2001). Regulation of intracellular trafficking of the EGF receptor by Rab5 in the absence of phosphatidylinositol 3-kinase activity. EMBO Rep. *2*, 68–74.

Chen, D., Fan, W., Lu, Y., Ding, X., Chen, S., and Zhong, Q. (2012). A mammalian autophagosome maturation mechanism mediated by TECPR1 and the Atg12-Atg5 conjugate. Mol. Cell *45*, 629–641.

Conroy, T., Desseigne, F., Ychou, M., Bouché, O., Guimbaud, R., Bécouarn, Y., Adenis, A., Raoul, J.L., Gourgou-Bourgade, S., de la Fouchardière, C., et al.; Groupe Tumeurs Digestives of Unicancer; PRODIGE Intergroup (2011). FOLFIRINOX versus gemcitabine for metastatic pancreatic cancer. N. Engl. J. Med. *364*, 1817–1825.

DeNicola, G.M., Karreth, F.A., Humpton, T.J., Gopinathan, A., Wei, C., Frese, K., Mangal, D., Yu, K.H., Yeo, C.J., Calhoun, E.S., et al. (2011). Oncogene-induced Nrf2 transcription promotes ROS detoxification and tumorigenesis. Nature *475*, 106–109.

Dinneen, J.L., and Ceresa, B.P. (2004). Expression of dominant negative rab5 in HeLa cells regulates endocytic trafficking distal from the plasma membrane. Exp. Cell Res. *294*, 509–522.

Eskelinen, E.L., Illert, A.L., Tanaka, Y., Schwarzmann, G., Blanz, J., Von Figura, K., and Saftig, P. (2002). Role of LAMP-2 in lysosome biogenesis and autophagy. Mol. Biol. Cell *13*, 3355–3368.

Feng, Z., Zhang, H., Levine, A.J., and Jin, S. (2005). The coordinate regulation of the p53 and mTOR pathways in cells. Proc. Natl. Acad. Sci. USA *102*, 8204–8209.

Frese, K.K., Neesse, A., Cook, N., Bapiro, T.E., Lolkema, M.P., Jodrell, D.I., and Tuveson, D.A. (2012). nab-Paclitaxel potentiates gemcitabine activity by reducing cytidine deaminase levels in a mouse model of pancreatic cancer. Cancer Discov. *2*, 260–269.

Furuta, N., Fujita, N., Noda, T., Yoshimori, T., and Amano, A. (2010). Combinational soluble N-ethylmaleimide-sensitive factor attachment protein receptor proteins VAMP8 and Vti1b mediate fusion of antimicrobial and canonical autophagosomes with lysosomes. Mol. Biol. Cell *21*, 1001–1010.

Galaviz-Hernandez, C., Stagg, C., de Ridder, G., Tanaka, T.S., Ko, M.S., Schlessinger, D., and Nagaraja, R. (2003). Plac8 and Plac9, novel placental-enriched genes identified through microarray analysis. Gene *309*, 81–89.

Ganley, I.G., Wong, P.M., Gammoh, N., and Jiang, X. (2011). Distinct autophagosomal-lysosomal fusion mechanism revealed by thapsigargin-induced autophagy arrest. Mol. Cell *42*, 731–743.

Guo, J.Y., Chen, H.Y., Mathew, R., Fan, J., Strohecker, A.M., Karsli-Uzunbas, G., Kamphorst, J.J., Chen, G., Lemons, J.M., Karantza, V., et al. (2011). Activated Ras requires autophagy to maintain oxidative metabolism and tumorigenesis. Genes Dev. *25*, 460–470.

Gutierrez, M.G., Munafó, D.B., Berón, W., and Colombo, M.I. (2004). Rab7 is required for the normal progression of the autophagic pathway in mammalian cells. J. Cell Sci. *117*, 2687–2697.

Hezel, A.F., Kimmelman, A.C., Stanger, B.Z., Bardeesy, N., and Depinho, R.A. (2006). Genetics and biology of pancreatic ductal adenocarcinoma. Genes Dev. *20*, 1218–1249.

Hidalgo, M. (2010). Pancreatic cancer. N. Engl. J. Med. *362*, 1605–1617.

Hingorani, S.R., Petricoin, E.F., Maitra, A., Rajapakse, V., King, C., Jacobetz, M.A., Ross, S., Conrads, T.P., Veenstra, T.D., Hitt, B.A., et al. (2003). Preinvasive and invasive ductal pancreatic cancer and its early detection in the mouse. Cancer Cell *4*, 437–450.

Hruban, R.H., Iacobuzio-Donahue, C., Wilentz, R.E., Goggins, M., and Kern, S.E. (2001). Molecular pathology of pancreatic cancer. Cancer J. *7*, 251–258.

Huynh, K.K., Eskelinen, E.L., Scott, C.C., Malevanets, A., Saftig, P., and Grinstein, S. (2007). LAMP proteins are required for fusion of lysosomes with phagosomes. EMBO J. *26*, 313–324.

Jäger, S., Bucci, C., Tanida, I., Ueno, T., Kominami, E., Saftig, P., and Eskelinen, E.L. (2004). Role for Rab7 in maturation of late autophagic vacuoles. J. Cell Sci. *117*, 4837–4848.

Jimenez-Preitner, M., Berney, X., Uldry, M., Vitali, A., Cinti, S., Ledford, J.G., and Thorens, B. (2011). Plac8 is an inducer of C/EBPβ required for brown fat differentiation, thermoregulation, and control of body weight. Cell Metab. *14*, 658–670.

Kimmelman, A.C. (2011). The dynamic nature of autophagy in cancer. Genes Dev. *25*, 1999–2010.

Kimura, S., Noda, T., and Yoshimori, T. (2007). Dissection of the autophagosome maturation process by a novel reporter protein, tandem fluorescent-tagged LC3. Autophagy *3*, 452–460.

Klionsky, D.J., Abeliovich, H., Agostinis, P., Agrawal, D.K., Aliev, G., Askew, D.S., Baba, M., Baehrecke, E.H., Bahr, B.A., Ballabio, A., et al. (2008). Guidelines for the use and interpretation of assays for monitoring autophagy in higher eukaryotes. Autophagy *4*, 151–175.

Klionsky, D.J., Abdalla, F.C., Abeliovich, H., Abraham, R.T., Acevedo-Arozena, A., Adeli, K., Agholme, L., Agnello, M., Agostinis, P., Aguirre-Ghiso, J.A., et al. (2012). Guidelines for the use and interpretation of assays for monitoring autophagy. Autophagy *8*, 445–544.

Komatsu, M., Waguri, S., Ueno, T., Iwata, J., Murata, S., Tanida, I., Ezaki, J., Mizushima, N., Ohsumi, Y., Uchiyama, Y., et al. (2005). Impairment of starvation-induced and constitutive autophagy in Atg7-deficient mice. J. Cell Biol. *169*, 425–434.

Kool, J., Uren, A.G., Martins, C.P., Sie, D., de Ridder, J., Turner, G., van Uitert, M., Matentzoglu, K., Lagcher, W., Krimpenfort, P., et al. (2010). Insertional mutagenesis in mice deficient for p15Ink4b, p16Ink4a, p21Cip1, and p27Kip1 reveals cancer gene interactions and correlations with tumor phenotypes. Cancer Res. *70*, 520–531.

Kuma, A., Hatano, M., Matsui, M., Yamamoto, A., Nakaya, H., Yoshimori, T., Ohsumi, Y., Tokuhisa, T., and Mizushima, N. (2004). The role of autophagy during the early neonatal starvation period. Nature *432*, 1032–1036.

Ledford, J.G., Kovarova, M., and Koller, B.H. (2007). Impaired host defense in mice lacking ONZIN. J. Immunol. *178*, 5132–5143.

Livesey, K.M., Kang, R., Vernon, P., Buchser, W., Loughran, P., Watkins, S.C., Zhang, L., Manfredi, J.J., Zeh, H.J., 3rd, Li, L., et al. (2012). p53/HMGB1 complexes regulate autophagy and apoptosis. Cancer Res. *72*, 1996–2005.

Lock, R., Roy, S., Kenific, C.M., Su, J.S., Salas, E., Ronen, S.M., and Debnath, J. (2011). Autophagy facilitates glycolysis during Ras-mediated oncogenic transformation. Mol. Biol. Cell *22*, 165–178.

Lowe, A.W., Olsen, M., Hao, Y., Lee, S.P., Taek Lee, K., Chen, X., van de Rijn, M., and Brown, P.O. (2007). Gene expression patterns in pancreatic tumors, cells and tissues. PLoS ONE *2*, e323.

Lüttges, J., Galehdari, H., Bröcker, V., Schwarte-Waldhoff, I., Henne-Bruns, D., Klöppel, G., Schmiegel, W., and Hahn, S.A. (2001). Allelic loss is often the first hit in the biallelic inactivation of the p53 and DPC4 genes during pancreatic carcinogenesis. Am. J. Pathol. *158*, 1677–1683.

McMurray, H.R., Sampson, E.R., Compitello, G., Kinsey, C., Newman, L., Smith, B., Chen, S.R., Klebanov, L., Salzman, P., Yakovlev, A., and Land, H. (2008). Synergistic response to oncogenic mutations defines gene class critical to cancer phenotype. Nature *453*, 1112–1116.

Mizushima, N., Sugita, H., Yoshimori, T., and Ohsumi, Y. (1998). A new protein conjugation system in human. The counterpart of the yeast Apg12p conjugation system essential for autophagy. J. Biol. Chem. *273*, 33889–33892.

Mizushima, N., Yamamoto, A., Hatano, M., Kobayashi, Y., Kabeya, Y., Suzuki, K., Tokuhisa, T., Ohsumi, Y., and Yoshimori, T. (2001). Dissection of autophagosome formation using Apg5-deficient mouse embryonic stem cells. J. Cell Biol. *152*, 657–668.

Morselli, E., Maiuri, M.C., Markaki, M., Megalou, E., Pasparaki, A., Palikaras, K., Criollo, A., Galluzzi, L., Malik, S.A., Vitale, I., et al. (2010). Caloric restriction and resveratrol promote longevity through the Sirtuin-1-dependent induction of autophagy. Cell Death Dis. *1*, e10.

Morselli, E., Shen, S., Ruckenstuhl, C., Bauer, M.A., Mariño, G., Galluzzi, L., Criollo, A., Michaud, M., Maiuri, M.C., Chano, T., et al. (2011). p53 inhibits autophagy by interacting with the human ortholog of yeast Atg17, RB1CC1/FIP200. Cell Cycle *10*, 2763–2769.

N'Diaye, E.N., Kajihara, K.K., Hsieh, I., Morisaki, H., Debnath, J., and Brown, E.J. (2009). PLIC proteins or ubiquilins regulate autophagy-dependent cell survival during nutrient starvation. EMBO Rep. *10*, 173–179.

O'Dell, M.R., Huang, J.L., Whitney-Miller, C.L., Deshpande, V., Rothberg, P., Grose, V., Rossi, R.M., Zhu, A.X., Land, H., Bardeesy, N., and Hezel, A.F. (2012). Kras(G12D) and p53 mutation cause primary intrahepatic cholangiocarcinoma. Cancer Res. *72*, 1557–1567.

Ogawa, M., Yoshikawa, Y., Kobayashi, T., Mimuro, H., Fukumatsu, M., Kiga, K., Piao, Z., Ashida, H., Yoshida, M., Kakuta, S., et al. (2011). A Tecpr1-dependent selective autophagy pathway targets bacterial pathogens. Cell Host Microbe *9*, 376–389.

Ohsumi, Y. (2001). Molecular dissection of autophagy: two ubiquitin-like systems. Nat. Rev. Mol. Cell Biol. *2*, 211–216.

Olive, K.P., Jacobetz, M.A., Davidson, C.J., Gopinathan, A., McIntyre, D., Honess, D., Madhu, B., Goldgraben, M.A., Caldwell, M.E., Allard, D., et al. (2009). Inhibition of Hedgehog signaling enhances delivery of chemotherapy in a mouse model of pancreatic cancer. Science *324*, 1457–1461.

Pimkina, J., and Murphy, M.E. (2009). ARF, autophagy and tumor suppression. Autophagy *5*, 397–399.

Provenzano, P.P., Cuevas, C., Chang, A.E., Goel, V.K., Von Hoff, D.D., and Hingorani, S.R. (2012). Enzymatic targeting of the stroma ablates physical barriers to treatment of pancreatic ductal adenocarcinoma. Cancer Cell *21*, 418–429.

Rhim, A.D., Mirek, E.T., Aiello, N.M., Maitra, A., Bailey, J.M., McAllister, F., Reichert, M., Beatty, G.L., Rustgi, A.K., Vonderheide, R.H., et al. (2012). EMT and dissemination precede pancreatic tumor formation. Cell *148*, 349–361.

Rogulski, K., Li, Y., Rothermund, K., Pu, L., Watkins, S., Yi, F., and Prochownik, E.V. (2005). Onzin, a c-Myc-repressed target, promotes survival and transformation by modulating the Akt-Mdm2-p53 pathway. Oncogene *24*, 7524–7541.

Rosenfeldt, M.T., O'Prey, J., Morton, J.P., Nixon, C., MacKay, G., Mrowinska, A., Au, A., Rai, T.S., Zheng, L., Ridgway, R., et al. (2013). p53 status determines the role of autophagy in pancreatic tumour development. Nature *504*, 296–300.

Rubinstein, A.D., Eisenstein, M., Ber, Y., Bialik, S., and Kimchi, A. (2011). The autophagy protein Atg12 associates with antiapoptotic Bcl-2 family members to promote mitochondrial apoptosis. Mol. Cell *44*, 698–709.

Smith, B., and Land, H. (2012). Anticancer activity of the cholesterol exporter ABCA1 gene. Cell Rep. *2*, 580–590.

Tanaka, Y., Guhde, G., Suter, A., Eskelinen, E.L., Hartmann, D., Lüllmann-Rauch, R., Janssen, P.M., Blanz, J., von Figura, K., and Saftig, P. (2000). Accumulation of autophagic vacuoles and cardiomyopathy in LAMP-2-deficient mice. Nature *406*, 902–906.

Tanida, I., Nishitani, T., Nemoto, T., Ueno, T., and Kominami, E. (2002). Mammalian Apg12p, but not the Apg12p.Apg5p conjugate, facilitates LC3 processing. Biochem. Biophys. Res. Commun. *296*, 1164–1170.

Tasdemir, E., Maiuri, M.C., Galluzzi, L., Vitale, I., Djavaheri-Mergny, M., D'Amelio, M., Criollo, A., Morselli, E., Zhu, C., Harper, F., et al. (2008). Regulation of autophagy by cytoplasmic p53. Nat. Cell Biol. *10*, 676–687.

White, E. (2012). Deconvoluting the context-dependent role for autophagy in cancer. Nat. Rev. Cancer *12*, 401–410.

Williams, G.T., Hughes, J.P., Stoneman, V., Anderson, C.L., McCarthy, N.J., Mourtada-Maarabouni, M., Pickard, M., Hedge, V.L., Trayner, I., and Farzaneh, F. (2006). Isolation of genes controlling apoptosis through their effects on cell survival. Gene Ther. Mol. Biol. *10* (B), 255–262.

Wong, S.H., Zhang, T., Xu, Y., Subramaniam, V.N., Griffiths, G., and Hong, W. (1998). Endobrevin, a novel synaptobrevin/VAMP-like protein preferentially associated with the early endosome. Mol. Biol. Cell *9*, 1549–1563.

Wu, S.F., Huang, Y., Hou, J.K., Yuan, T.T., Zhou, C.X., Zhang, J., and Chen, G.Q. (2010). The downregulation of onzin expression by PKCepsilon-ERK2 signaling and its potential role in AML cell differentiation. Leukemia *24*, 544–551.

Xia, M., and Land, H. (2007). Tumor suppressor p53 restricts Ras stimulation of RhoA and cancer cell motility. Nat. Struct. Mol. Biol. *14*, 215–223.

Yamamoto, A., Tagawa, Y., Yoshimori, T., Moriyama, Y., Masaki, R., and Tashiro, Y. (1998). Bafilomycin A1 prevents maturation of autophagic vacuoles by inhibiting fusion between autophagosomes and lysosomes in rat hepatoma cell line, H-4-II-E cells. Cell Struct. Funct. *23*, 33–42.

Yang, S., Wang, X., Contino, G., Liesa, M., Sahin, E., Ying, H., Bause, A., Li, Y., Stommel, J.M., Dell'antonio, G., et al. (2011). Pancreatic cancers require autophagy for tumor growth. Genes Dev. *25*, 717–729.

Ying, H., Kimmelman, A.C., Lyssiotis, C.A., Hua, S., Chu, G.C., Fletcher-Sananikone, E., Locasale, J.W., Son, J., Zhang, H., Coloff, J.L., et al. (2012). Oncogenic Kras maintains pancreatic tumors through regulation of anabolic glucose metabolism. Cell *149*, 656–670.